A Local Representation of the Electronic Dielectric Response Function

Xiaochuan Ge[1] and Deyu Lu[1, *]

[1]Center for Functional Nanomaterials, Brookhaven National Laboratory , Upton, New York 11973, United States
(Dated: June 19, 2017)

We present a local representation of the electronic dielectric response function, based on a spatial partition of the dielectric response into contributions from each Wannier function using a generalized density functional perturbation theory. This procedure is fully *ab initio*, and therefore allows us to rigorously define local metrics, such as "bond polarizability", on Wannier centers. We show that the locality of the response function is determined by the locality of three quantities: Wannier functions of the occupied manifold, the density matrix, and the Hamiltonian matrix. In systems with a gap, the bare dielectric response is exponentially localized, which supports the physical picture of the dielectric response function as a collection of interacting local response that can be captured by a tight-binding model.

The screened electronic dielectric response function (EDRF), χ, is a fundamental physical quantity that captures many-electron correlation effects. From a microscopic point of view, χ relates the perturbation from an external potential at $\mathbf{r}'$ to the electronic density response at $\mathbf{r}$. This intrinsic non-local character has precluded a compact local representation of χ in electronic structure theory; it has been traditionally represented by huge matrices in either real or reciprocal space [1]. This cumbersome matrix representation of χ has become a major computational bottleneck to accurately predict electron correlation energy and electronic excitation spectra. More importantly, the physical interpretation of χ is largely limited to its macroscopic average. A robust, microscopic theory that describes the local characteristics (e.g., shape, strength and decay rate) is needed to unravel the underlying physical nature of EDRFs.

Empirical methods have been used to partition EDRFs to obtain polarizabilities or effective van der Waals C_6 dispersion coefficients of atoms inside either a molecule or a solid [2, 3]. On the other hand, non-empirical methods often rely on extra approximations to partition, e.g., the molecular polarizability, into so-called "distributed polarizabilities" [4]. Such procedures typically involve partitioning the volume [5] or the basis space [6] of a molecule, or fitting the point-to-point polarizabilities computed on a grid around a molecule [7], with known drawbacks including large charge-flow terms that are hard to localize, strong basis set dependence, and high computational cost [8].

The Wannier function (WF) representation [9] is a natural choice to describe chemical bonds using either "Boys orbitals" for molecules [10] or the maximally localized Wannier functions (MLWFs) for the solid-state equivalent [11–13]. However, the link between local EDRFs and WFs is obscured by the fact that EDRFs concern electron-hole pairs rather than electronic orbitals alone. Silvestrelli [14] proposed to define C_6 coefficients on Wannier centers using empirical models, assuming that WFs

have the s-symmetry. Giustino and Pasquarello [15] introduced the local dielectric permittivity in layered systems, based on local dipole moments derived from each Wannier function using the Berry-phase theory of the polarization [16]. However, this approach requires separate calculations under finite external fields, unsuitable to study the spatial decay rate and the dynamic response. Lu *et al.* [17] applied a simultaneous diagonalization algorithm to directly localize the eigenvectors of EDRFs. Despite the observed trend in the locality [17], the chemical nature of localized EDRFs was not determined precisely.

In this Letter, we propose a local representation for microscopic EDRFs using a generalized density functional perturbation theory (DFPT) [18]. While the conventional theory is formulated on the eigenstates of the Kohn-Sham (KS) Hamiltonian, we generalize the DFPT to any orthogonal basis set that spans the occupied state manifold. A convenient choice adopted in this work is the MLWF [11, 12], as it can provide insightful interpretations regarding chemical bonds. Because this method is fully *ab initio*, it ensures accuracy and transferability.

First we generalize DFPT for the bare EDRF, χ^0, which is the building block in linear response theory. Under a perturbation in the self-consistent potential, $e^{-i\omega t}\Delta V_s(\mathbf{r})$, the response density can be calculated through χ^0 as

$$\Delta\rho(\omega;\mathbf{r}) = \int d\mathbf{r}' \, \chi^0(\omega;\mathbf{r},\mathbf{r}') \, \Delta V_s(\mathbf{r}'). \qquad (1)$$

In the following, we adopt the shorthand notation: $\Delta\rho = \chi^0 \Delta V_s$. χ can be solved from χ^0 through Dyson's equation, $\chi = \chi^0 + \chi^0 K \chi$, where $K = v_c + K_{xc}$ with v_c and K_{xc} being Coulomb and exchange-correlation kernels, respectively [19]. For periodic systems, Eq. 1 is often solved for individual Fourier components with wave vectors $\mathbf{q}$, $\Delta V_s^{\mathbf{q}}(\mathbf{r}) = e^{i\mathbf{q}\cdot\mathbf{r}}\Delta v_s(\mathbf{r})$. The response density matrix is given by

$$\Delta\rho_{\mathbf{q}} = \frac{2}{\Omega}\sum_{v\mathbf{k}} \left|\Delta\psi_{v\pm}^{\mathbf{k}+\mathbf{q}}\right\rangle \left\langle\psi_v^{\mathbf{k}}\right|, \qquad (2)$$

where the variation of the KS orbital, $|\Delta\psi_{v\pm}^{\mathbf{k}+\mathbf{q}}\rangle$, is the solution of the Sternheimer equation [18],

$$(\varepsilon_v^{\mathbf{k}} - H - \alpha P_v^{\mathbf{k}+\mathbf{q}} \pm \omega)\left|\Delta\psi_{v\pm}^{\mathbf{k}+\mathbf{q}}\right\rangle = P_c^{\mathbf{k}+\mathbf{q}}\Delta V_s^{\mathbf{q}}\left|\psi_v^{\mathbf{k}}\right\rangle. \quad (3)$$

Here $\alpha P_v^{\mathbf{k}+\mathbf{q}}$ makes Eq. 3 non singular; $P_v^{\mathbf{k}+\mathbf{q}}$ and $P_c^{\mathbf{k}+\mathbf{q}}$ are projectors onto the occupied and unoccupied state manifolds at momentum $\mathbf{k}+\mathbf{q}$, which are introduced to avoid the explicit reference to the unoccupied states [18].

It is trivial to partition $\Delta\rho_{\mathbf{q}}$ in Eq. 2 in the energy domain into contributions from individual KS orbitals at given $\{v, \mathbf{k}\}$ and $\mathbf{q}$, and the corresponding linear equations in Eq. 3 are decoupled. Alternatively, a real space partition of EDRFs can be achieved through a generalized DFPT in the WF representation. Following the notations in Ref. [11], we define WFs and their first order perturbations as

$$W_{\mathbf{R}n}(\mathbf{r}) = \frac{\Omega}{(2\pi)^3}\int_{BZ}d\mathbf{k}e^{-i\mathbf{k}\cdot\mathbf{R}}\sum_{m=1}^{J}U_{mn}^{(\mathbf{k})}\psi_m^{\mathbf{k}}(\mathbf{r}),$$

$$\Delta W_{\mathbf{R}n}^{\pm}(\mathbf{r}) = \frac{\Omega}{(2\pi)^3}\int_{BZ}d\mathbf{k}e^{-i\mathbf{k}\cdot\mathbf{R}}\sum_{\mathbf{q}}\sum_{m=1}^{J}U_{mn}^{(\mathbf{k})}\Delta\psi_{m\pm}^{\mathbf{k}+\mathbf{q}}(\mathbf{r}),$$
$$(4)$$

where J is the number of orbitals used to construct WFs, and unitary matrices $U^{(\mathbf{k})}$ minimize the spatial spreads of the WFs labeled by lattice vector $\mathbf{R}$ and band index n [11]. For simplicity, we will focus on the the static limit and drop the superscripts $+$ and $-$; extension to the dynamic case is straightforward. Because ρ and, thus, $\Delta\rho$ are invariant under the unitary transformation of occupied states, Eq. 2 can be rewritten in the Wannier representation as

$$\Delta\rho = \frac{4}{\Omega}\sum_{\mathbf{R}n}|\Delta W_{\mathbf{R}n}\rangle\langle W_{\mathbf{R}n}|. \quad (5)$$

Applying $U^{(\mathbf{k})}$ to both sides of Eq. 3 and integrating over $\mathbf{k}$, one obtains the generalized Sternheimer equation in the Wannier representation as

$$\sum_{\mathbf{R}'n'}(\tilde{\varepsilon}_{\mathbf{R}n,\mathbf{R}'n'} - H - \alpha P_v)|\Delta W_{\mathbf{R}'n'}\rangle = P_c\Delta V_s|W_{\mathbf{R}n}\rangle. \quad (6)$$

Because WFs are not eigenstates of the KS Hamiltonian, unlike Eq. 3, Eq. 6 yields a set of coupled equations due to the hopping integral terms, $\tilde{\varepsilon}_{\mathbf{R}n,\mathbf{R}'n'} = \langle W_{\mathbf{R}n}|H|W_{\mathbf{R}'n'}\rangle$ ($\mathbf{R}n \neq \mathbf{R}'n'$). It follows that

$$|\Delta W_{\mathbf{R}n}\rangle = \sum_{\mathbf{R}'n'}|\Delta W_{\mathbf{R}n,\mathbf{R}'n'}\rangle$$
$$\equiv \sum_{\mathbf{R}'n'}[\tilde{\varepsilon} - (H + \alpha P_v)\,I]_{\mathbf{R}n,\mathbf{R}'n'}^{-1}P_c\Delta V_s|W_{\mathbf{R}'n'}\rangle, \quad (7)$$

where I is an $N_W \times N_W$ identity matrix with N_W being the number of occupied WFs. $\Delta W_{\mathbf{R}n,\mathbf{R}'n'}$ denotes

the variation of $W_{\mathbf{R}n}$ caused by the perturbation at $W_{\mathbf{R}'n'}$. Combining Eqs. 5 and 7, one can expand χ^0 in terms of two-body partial response functions, $\chi^0 = \sum_{\mathbf{R}n,\mathbf{R}'n'}\chi^0_{\mathbf{R}n,\mathbf{R}'n'}$, with corresponding density response given by $\Delta\rho_{\mathbf{R}n,\mathbf{R}'n'} \equiv \frac{4}{\Omega}|\Delta W_{\mathbf{R}n,\mathbf{R}'n'}\rangle\langle W_{\mathbf{R}n}|$. A formal real space partition can be established by contracting $\chi^0_{\mathbf{R}n,\mathbf{R}'n'}$ into one-body variables,

$$\chi^0(\mathbf{r},\mathbf{r}') = \sum_{\mathbf{R}n}\chi^0_{\mathbf{R}n}(\mathbf{r},\mathbf{r}'),$$

$$\chi^0_{\mathbf{R}n}(\mathbf{r},\mathbf{r}') = \frac{1}{2}\sum_{\mathbf{R}'n'}\left[\chi^0_{\mathbf{R}n,\mathbf{R}'n'}(\mathbf{r},\mathbf{r}') + \chi^0_{\mathbf{R}'n',\mathbf{R}n}(\mathbf{r},\mathbf{r}')\right].$$
$$(8)$$

$\chi^0_{\mathbf{R}n}$ is Hermitian by construction. It contains not only on-site terms, but also the charge-flow ($\mathbf{R}'n' \neq \mathbf{R}n$) into and out of the local orbital, whose magnitude determines the extent of the locality of χ^0. Eq. 8 is the central equation of our theory, which together with the locality analysis below formally establishes the local representation of EDRFs. The real space partition can be achieved similarly for χ through partial response functions, $\chi_{\mathbf{R}n} = \frac{1}{2}\sum_{\mathbf{R}'n'}(\chi_{\mathbf{R}n,\mathbf{R}'n'} + \chi_{\mathbf{R}'n',\mathbf{R}n})$, where

$$\chi_{\mathbf{R}n,\mathbf{R}'n'} = \sum_{\mathbf{R}''n''}\sum_{m=0}^{\infty}\chi^0_{\mathbf{R}n,\mathbf{R}''n''}\left(K\chi^0\right)^m_{\mathbf{R}''n'',\mathbf{R}'n'},$$

$$\chi_{\mathbf{R}'n',\mathbf{R}n} = \sum_{\mathbf{R}''n''}\sum_{m=0}^{\infty}\left(\chi^0 K\right)^m_{\mathbf{R}'n',\mathbf{R}''n''}\chi^0_{\mathbf{R}''n'',\mathbf{R}n},(9)$$

are solved self-consistently with Eq. 6. We emphasize that there is a critical distinction between Eqs. 8-9 and existing approximate partition methods. In our method, once a Wannier localization procedure is chosen, the subsequent real space EDRF partition is exact.

To demonstrate the concept of the local EDRF, we partition static molecular polarizabilities of acetylene (C_2H_2), ethylene (C_2H_4), and ethane (C_2H_6) into bond polarizabilities at Wannier centers. The major difference between these molecules is the C-C bond order: single bond in C_2H_6, double bond in C_2H_4, and triple bond in C_2H_2. We compare the standard mean screened polarizability ($\bar{\alpha} = \frac{1}{3}tr(\hat{\mathbf{r}}\chi\hat{\mathbf{r}}')$) with the unscreened one ($\bar{\alpha}^0 = \frac{1}{3}tr(\hat{\mathbf{r}}\chi^0\hat{\mathbf{r}}')$) to gain insight into the local field effect. All the calculations were performed at the random phase approximation level using Wannier90 [20] and a modified version of QUANTUM ESPRESSO [21]; computational details are given in the Supplemental Material (SM) [22].

Within C_2H_2, as shown in Table I, $\bar{\alpha}^0(\pi_{CC}) > \bar{\alpha}^0(CH) > \bar{\alpha}^0(\sigma_{CC})$. This behavior is a direct outcome of the electronic structure, because π_{CC} is closest to the lowest unoccupied molecular orbital (LUMO) in energy (i.e., most reactive), and σ_{CC} is farthest from LUMO (i.e., least reactive) as shown by the projected density of states in Fig. S2 in SM. The same trend holds for all three molecules. Among different molecules, unscreened bond

TABLE I: Mean static molecular and bond polarizabilities (in Bohr^3) of C_2H_6, C_2H_4, and C_2H_2. Multipliers in bond polarizabilities indicate the degeneracy; unscreened bond polarizabilities are shown in the parentheses.

	Total	C-H	C-C	σ_{CC}	π_{CC}
C_2H_2	24.65	2×3.11(4.36)	18.43	0.60(1.55)	2×8.92(16.26)
C_2H_4	29.41	4×3.91(5.73)	13.76	1.73(3.30)	12.02(21.28)
C_2H_6	31.35	6×4.54(6.60)	4.09	4.09(6.25)	

polarizabilities increase in the order of C_2H_2, C_2H_4, and C_2H_6, partially due to the reduced bonding-antibonding splitting with increased bond lengths (d_{CH}: 1.000, 1.018, 1.024; d_{CC}: 1.000, 1.102, 1.267, both normalized by the bond lengths of C_2H_2). Another dominating factor in the molecular polarizability is the number of bonds, i.e., the degeneracy. On the other hand, $\bar{\alpha}$ is always smaller than $\bar{\alpha}^0$, because of the screening effect. We define $\epsilon_{eff} = \bar{\alpha}^0/\bar{\alpha}$ as a measure of the local screening strength that includes both intra- and inter-bond screening effects. ϵ_{eff} is highly heterogeneous in these molecules, and the largest values arise from the strongly overlapping σ_{CC} and π_{CC} bonds. Consequently, $\epsilon_{eff}(\sigma_{CC})$ (1.9 and 2.6) and $\epsilon_{eff}(\pi_{CC})$ (1.8) in C_2H_2 and C_2H_4 are significantly larger than $\epsilon_{eff}(\sigma_{CH})$ (1.4 ~ 1.5) and $\epsilon_{eff}(\sigma_{CC})$ in C_2H_6 (1.5).

For systems with a finite gap, it has been proved that (a) $W_{\mathbf{R}n}(\mathbf{r})$ decays exponentially with $|\mathbf{r}-\mathbf{R}|$ [23, 24]; (b)
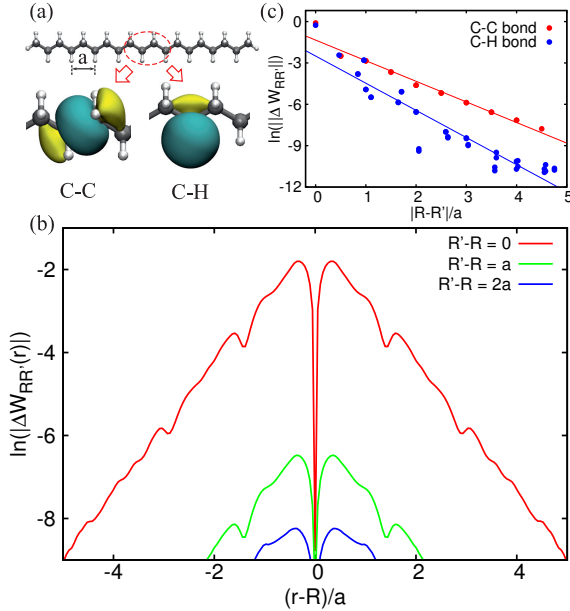

FIG. 1: Locality of $\Delta W_{\mathbf{RR}'}(\mathbf{r})$ in an ethylene oligomer ($C_{19}H_{40}$). (a) Wannier orbitals of C-C and C-H bonds. (b) The exponential decay of $\Delta W_{\mathbf{RR}'}(\mathbf{r})$ as a function of $|\mathbf{r} - \mathbf{R}'|$ (only shown for C-H bond) and (c) of $||\Delta W_{\mathbf{RR}'}||$ as a function of $|\mathbf{R} - \mathbf{R}'|$. Solid lines in (c) indicate a linear fit.
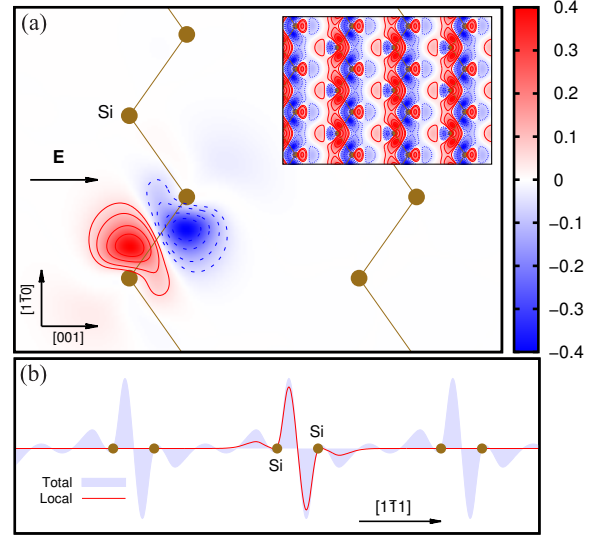

FIG. 2: The (local) density response of silicon under a uniform electronic field in the [001] direction. (a) Contour plot of the local density response in the [110] plane of a Si-Si bond (inset: total density response). (b) Density response profile along the Si-Si bond.

the Hamiltonian matrix $\tilde{\varepsilon}_{\mathbf{R}n,\mathbf{R}'n'}$ decays exponentially with $|\mathbf{R} - \mathbf{R}'|$ [25]; and (c) the density matrix $\langle\mathbf{r}|P_v|\mathbf{r}'\rangle$ decays exponentially with $|\mathbf{r} - \mathbf{r}'|$ [25–27]. The locality of $\Delta W_{\mathbf{R}n,\mathbf{R}'n'}(\mathbf{r})$ can be derived accordingly. (i) For a regular potential that is not exponentially divergent, $P_c \Delta V_s W_{\mathbf{R}'n'}(\mathbf{r})$ decays exponentially with $|\mathbf{r} - \mathbf{R}'|$. This can be easily understood from the locality of $W_{\mathbf{R}n}(\mathbf{r})$ and P_v, as $P_c = I - P_v$. (ii) $[\tilde{\varepsilon} - (H + \alpha P_v)I]^{-1}_{\mathbf{RR}'}$ decays exponentially with $|\mathbf{R} - \mathbf{R}'|$, a direct consequence of the locality of $\tilde{\varepsilon}_{\mathbf{R}n,\mathbf{R}'n'}$ [34]. (iii) Putting (i) and (ii) together, we conclude that $\Delta W_{\mathbf{R}n,\mathbf{R}'n'}(\mathbf{r})$ decays exponentially with $|\mathbf{r} - \mathbf{R}'|$ for a given $\mathbf{R}$ and $\mathbf{R}'$ pair, and its two-norm, $||\Delta W_{\mathbf{R}n,\mathbf{R}'n'}|| = \sqrt{\int d\mathbf{r}|\Delta W_{\mathbf{R}n,\mathbf{R}'n'}(\mathbf{r})|^2}$, decays exponentially with $|\mathbf{R} - \mathbf{R}'|$.

To validate these arguments, we considered an ethylene oligomer ($C_{19}H_{40}$ with unit length a) containing two types of WFs, C-C and C-H bonds, as shown in Fig. 1a. To quantify the locality of $\Delta W_{\mathbf{R}n\mathbf{R}'n'}$, we consider a linear potential $V_s(\mathbf{r}) = x$ applied along the molecule. Both $\Delta W_{\mathbf{R}n\mathbf{R}'n'}(\mathbf{r})$ (Fig. 1b) and $||\Delta W_{\mathbf{R}n,\mathbf{R}'n'}||$ (Fig. 1c) clearly exhibit an exponential decay. While the decay length of the former (0.6 ~ 1.0a) is governed by the locality of the WFs (0.3 ~ 0.5a) and the density matrix, the latter (0.5 ~ 0.7a) is controlled by the locality of $\tilde{\varepsilon}_{\mathbf{R}n\mathbf{R}'n'}$ (see Fig. S4 in SM).

The strong spatial localization of the response density also exists in 3D crystals, as shown in bulk silicon in Fig. 2. Under a uniform electronic field, although the total response density is delocalized, 82% local density response along the [1$\bar{1}$1] direction is confined within one Si-Si bond (see Fig. 2b).

An important outcome of the exponential localization of $W_{\mathbf{R}n}(\mathbf{r})$ and $\Delta W_{\mathbf{R}n,\mathbf{R}'n'}(\mathbf{r})$ is that $\chi^0_{\mathbf{R}n,\mathbf{R}'n'}$ is exponentially localized. It supports the physical picture of χ^0 as a linear combination of coupled local response modes centered on WFs. Consequently, efficient algorithms can be developed to compute χ^0, taking advantage of its sparse representation in the real space. To prove this point, we construct a tight-binding model of χ^0 for silicon with a local basis set, and compute its eigenvalue spectrum in the Brillouin zone using the dielectric band structure (DBS) interpolation, in analogy to the electronic band structure interpolation using Wannier functions [12]. To our best knowledge, this is the first demonstration of DBS interpolation for a covalent bonded crystal.

We first construct local basis set of χ^0 denoted by $\left|\xi_i^{\mathbf{R}n}\right\rangle$, as approximate eigenvectors of $\chi^0_{\mathbf{R}n\mathbf{R}n}$, where hopping terms $\tilde{\epsilon}_{\mathbf{R}n,\mathbf{R}'n'}$ ($\mathbf{R}n \neq \mathbf{R}'n'$) are switched off. This procedure decouples equations in Eq. 6, making them easy to solve computationally. Then we calculate the hopping matrix X and overlap matrix S in real space, $X_{ij}^{nn'}(\mathbf{R}) = \left\langle\xi_i^{0n}|\chi^0|\xi_j^{\mathbf{R}n'}\right\rangle$, and $S_{ij}^{nn'}(\mathbf{R}) = \left\langle\xi_i^{0n}|\xi_j^{\mathbf{R}n'}\right\rangle$. Finally we Fourier transform them into momentum space,

$$
\begin{aligned}
\tilde{X}(\mathbf{q}) &= \sum_{\mathbf{R}} X(\mathbf{R})e^{i\mathbf{q}\cdot\mathbf{R}}, \\
\tilde{S}(\mathbf{q}) &= \sum_{\mathbf{R}} S(\mathbf{R})e^{i\mathbf{q}\cdot\mathbf{R}}.
\end{aligned} \tag{10}
$$

The interpolated DBS of χ^0 is the solution of the generalized eigenvalue problem in non-orthogonal basis:

$$
\tilde{X}(\mathbf{q})\vec{v} = \lambda(\mathbf{q})\tilde{S}(\mathbf{q})\vec{v}. \tag{11}
$$

We demonstrated the DBS interpolation method with bulk silicon using a $4 \times 4 \times 4$ k-mesh for the direct calculation, and a $4 \times 4 \times 4$ super cell with Γ-point sampling to construct the local basis set, X and S in real space [35]. Twenty five local eigenmodes per WF are sufficient to reach the numerical convergence of the first 25 bands of the total χ^0. The Wannier orbitals and the first ten dielectric basis functions of bulk silicon are shown in Fig. 3a and 3b. Excellent agreement (maximum absolute error: $2.6 \times 10^{-4} a.u.$) was found between the direct calculation and interpolated DBS in Fig. 3c, which highlights the validity and accuracy of the tight-binding model of χ^0.

The local basis set is the key to the efficient construction of χ^0. Thanks to the exponential localization of $\chi^0_{\mathbf{R}n,\mathbf{R}'n'}$, Eq. 6 in principle can be solved within a subspace containing n_n neighboring Wannier orbitals of the local perturbation. Since n_n is system size independent, the computational cost grows as $O(N^2 ln(N))$ with N being the size of the system, which is a tremendous improvement over the standard $O(N^4)$ scaling (see SM). This quadratic scaling method is a promising starting point to develop low scaling algorithms for excited state
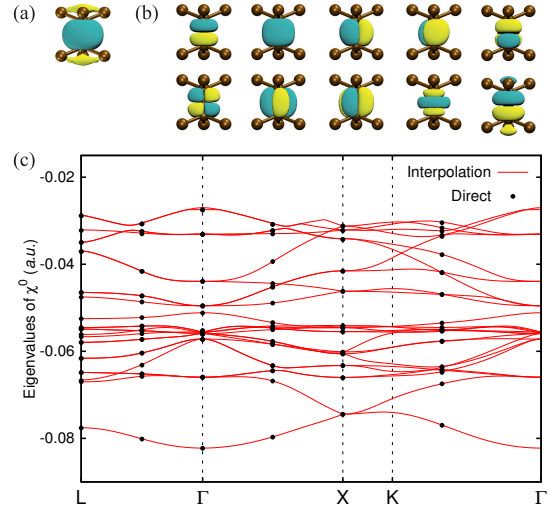

FIG. 3: DBS (χ^0) interpolation for bulk silicon using local basis. (a) The WF in bulk silicon. (b) The first 10 eigenmodes of the local response function. (c) Comparison of the DBS obtained from a direct calculation with interpolation using the lowest 25 basis functions per WF.

problems, where the evaluation of χ^0 is the major bottleneck to construct, e.g., $\epsilon_{RPA} = 1 - v\chi^0$ or χ [28–30].

The theoretical framework of local EDRFs can be extended to metallic systems, as DFPT can treat metallic systems in general [18], but the decay rate of key quantities can behave qualitatively differently from semiconductors or insulators. In 1D free electrons, the Wannier orbital of the occupied portion of bands decays at r^{-1} [25]. For Wannier orbitals of disentangled bands, e.g., narrow transition metal d-bands, both numerical evidence and the analogy with the isolated composite case suggest the possibility of the exponential localization [13]. On the other hand, the decay of density matrix is expected to be algebraic at zero temperature, and exponential at finite temperature [26, 27]. The locality of EDRFs in metallic systems is therefore more subtle, and warrants further investigation.

In conclusion, we present a local representation of EDRFs based on the concept of the dielectric response of WFs. This method allows us to perform fully *ab initio* real space partition of EDRFs, and analyze excited state properties, e.g., polarizability, in terms of chemical bonds. In systems with a gap, we proved that the bare response function, $\chi^0_{\mathbf{R}n,\mathbf{R}'n'}$, decays exponentially in real space. This "near-sightness" is central to the physical understanding of EDRFs and the development of low scaling algorithms for excited state problems.

* Electronic address: dlu@bnl.gov

[1] G. Onida, L. Reining, and A. Rubio, Rev. Mod. Phys. **74**, 601 (2002).

[2] Q. Wu and W. Yang, J. Chem. Phys. **116**, 515 (2002).

[3] A. Tkatchenko and M. Scheffler, Phys. Rev. Lett. **102**, 6 (2009).

[4] A. Stone, Mol. Phys. **56**, 1065 (1985).

[5] J. G. Ángyán, G. Jansen, M. Loss, C. Hättig, and B. A. Heß, Chem. Phys. Lett. **219**, 267 (1994).

[6] C. R. Le Sueur and A. J. Stone, Mol. Phys. **78**, 1267 (1993).

[7] G. J. Williams and A. J. Stone, J. Chem. Phys. **119**, 4620 (2003).

[8] A. J. Misquitta and A. J. Stone, J. Chem. Phys. **124**, 024111 (2006).

[9] G. H. Wannier, Phys. Rev. **52**, 191 (1937).

[10] S. F. Boys, Rev. Mod. Phys. **32**, 296 (1960).

[11] N. Marzari and D. Vanderbilt, Phys. Rev. B **56**, 12847 (1997).

[12] I. Souza, N. Marzari, and D. Vanderbilt, Phys. Rev. B **65**, 035109 (2001).

[13] N. Marzari, A. A. Mostofi, J. R. Yates, I. Souza, and D. Vanderbilt, Rev. Mod. Phys. **84**, 1419 (2012).

[14] P. L. Silvestrelli, Phys. Rev. Lett. **100**, 053002 (2008).

[15] F. Giustino and A. Pasquarello, Phys. Rev. B **71**, 144104 (2005).

[16] R. Resta, Rev. Mod. Phys. **66**, 899 (1994).

[17] D. Lu, F. Gygi, and G. Galli, Phys. Rev. Lett. **100**, 147601 (2008).

[18] S. Baroni, S. de Gironcoli, A. Dal Corso, and P. Giannozzi, Rev. Mod. Phys. **73**, 515 (2001).

[19] A. L. Fetter and J. D. Walecka, *Quantum theory of many-particle systems* (Courier Corporation, 2003).

[20] A. A. Mostofi *et al.*, Comput. Phys. Commun. **178**, 685 (2008).

[21] P. Giannozzi *et al.*, J. Phys.: Condens. Matter **21**, 395502 (2009).

[22] Suplemental Material: [URL to beinserted by publisher].

[23] W. Kohn, Phys. Rev. **115**, 809 (1959).

[24] G. Panati and A. Pisante, Commun. Math. Phys. **322**, 835 (2013).

[25] L. He and D. Vanderbilt, Phys. Rev. Lett. **86**, 5341 (2001).

[26] S. Goedecker, Phys. Rev. B **58**, 3501 (1998).

[27] S. Ismail-Beigi and T. A. Arias, Phys. Rev. Lett. **82**, 2127 (1999).

[28] D. Lu, Y. Li, D. Rocca, and G. Galli, Phys. Rev. Lett. **102**, 206411 (2009).

[29] P. Umari, G. Stenuit, and S. Baroni, Phys. Rev. B **81**, 115104 (2010).

[30] D. Rocca, D. Lu, and G. Galli, J. Chem. Phys. **133**, (2010).

[31] S. Demko, W. F. Moss, and P. W. Smith, Math. Comp. **43**, 491 (1984).

[32] S. L. Adler, Phys. Rev. **126**, 413 (1962).

[33] N. Wiser, Phys. Rev. **129**, 62 (1963).

[34] Since its off-diagonal elements decay exponentially with distance, $\tilde{\varepsilon}$ can be truncated beyond the distance that is several times of the decay length, so that $(H + \alpha P_v)I - \tilde{\varepsilon}$ becomes a positive definite block banded matrix. It has been proved that the inverse of such a matrix has exponentially decayed off-diagonal elements [31].

[35] We have verified that a k-point implementation of DBS interpolation with a $4 \times 4 \times 4$ k-mesh would yield the same results, although the Γ-point implementation is more straightforward.

A Local Representation of the Electronic Dielectric Response Function
Supplemental Material

Xiaochuan Ge[1] and Deyu Lu[1]

[1]*Center for Functional Nanomaterials, Brookhaven National Laboratory , Upton, New York 11973, United States*
(Dated: June 19, 2017)

ELECTRONIC STRUCTURE OF C_2H_n, $(n = 2, 4, 6)$

The polarizability decomposition of acetylene (C_2H_2), ethylene (C_2H_4), and ethane (C_2H_6) was performed with Wannier90 [1] and a modified version of QUANTUM ESPRESSO [2] using the Perdew-Zunger functional [3] in a $35 \times 18 \times 18$ a_0^3 super-cell. The norm-conserving pseudo potential was used with energy cutoffs of 40 and 160 Ry for the wavefunction and charge density, respectively. The maximally localized Wannier functions (MLWFs) of these molecules are shown in Fig. S1. For C_2H_2 and C_2H_4, a regular construction of WFs results in a mixture of π and σ bonds. Instead, σ (from p_x) and π (from p_y and p_z) orbitals were constructed separately, where x is along the direction of the C-C bond.
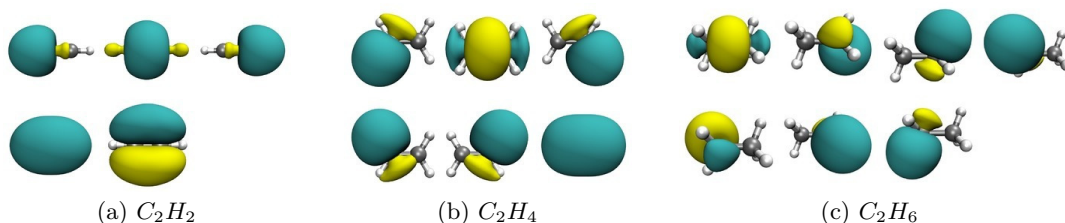

(a) C_2H_2 (b) C_2H_4 (c) C_2H_6

FIG. S1: The WFs of C_2H_2 (two π_{CC} and one σ_{CC} bonds), C_2H_4 (one π_{CC} and one σ_{CC} bonds), and C_2H_6 (one σ_{CC} bond).

The magnitude of the unscreened bond polarizability $(\bar{\alpha}^0)$ is inversely related to the transition energy (ΔE) between the occupied states and the onset of the unoccupied manifold, i.e., the lowest unoccupied molecular orbital (LUMO). The relative energy of different chemical bonds is indicated in the projected density of states (PDOS) onto Wannier orbitals in Fig. S2. Since WFs are not eigenfunctions of the Kohn-Sham Hamiltonian, their PDOS can spread in an energy range, making it hard to compare between different WFs. Here we define the average energy of a WF as the on-site Hamiltonian matrix element, $\langle W_n|H|W_n \rangle$, indicated by the colored dashed lines in Fig. S2. Within the same molecule, in average $\Delta E(\pi_{CC}) < \Delta E(CH) < \Delta E(\sigma_{CC})$, which implies that $\bar{\alpha}^0(\pi_{CC}) > \bar{\alpha}^0(CH) > \bar{\alpha}^0(\sigma_{CC})$. It also explains the increasing order of bond polarizabilities in C_2H_2, C_2H_4, and C_2H_6 for the same kind of bonds.
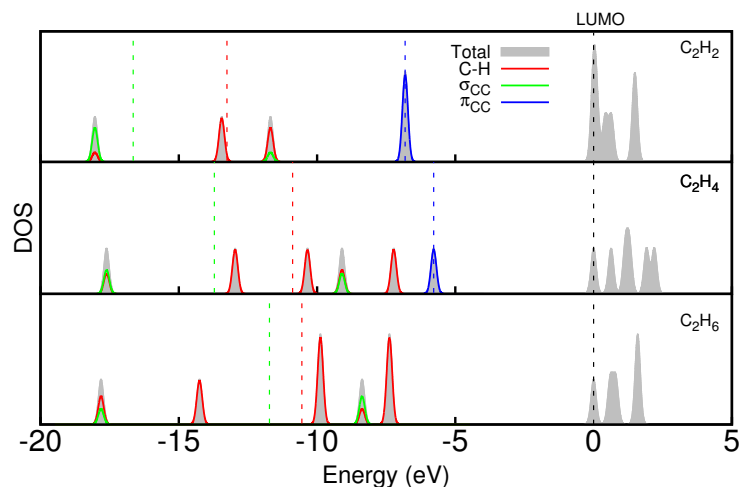

FIG. S2: Density of states projected onto WFs of C_2H_2, C_2H_4, and C_2H_6. Colored dashed lines indicate the average energy levels of Wannier orbitals.

LOCALITY OF THE RESPONSE OF WANNIER FUNCTIONS

The locality of $\Delta W_{\mathbf{R}n,\mathbf{R}'n'}(\mathbf{r})$ has two meanings as described in the main text. First $\Delta W_{\mathbf{R}n,\mathbf{R}'n'}(\mathbf{r})$ decays exponentially with $|\mathbf{r} - \mathbf{R}'|$ for a given pair of $\mathbf{R}$ and $\mathbf{R}'$. Second the two-norm, $||\Delta W_{\mathbf{R}n,\mathbf{R}'n'}||$, decays exponentially with $|\mathbf{R} - \mathbf{R}'|$.

In fact, the first locality is closely related to that of the WFs and the density matrix. As shown in Fig. S3, the quantity $F(\mathbf{r}) = P_c \Delta V_s W_{Rn}(\mathbf{r})$ exponentially decays in the real space, and the decay length ($0.6a$ and $1.0a$ for C-H and C-C bonds, respectively) is approximately twice as its corresponding WF ($0.3a$ and $0.5a$ for C-H and C-C bonds, respectively, not shown). This is because the projector, $P_c(\mathbf{r}, \mathbf{r}') = I - P_v(\mathbf{r}, \mathbf{r}')$, has a similar decay length as the WF, therefore broadens the spread of the WF by two in $F(\mathbf{r})$. Comparing Fig. S3 and Fig. 1b in the main text, we observe that the locality of $\Delta W_{\mathbf{R}n\mathbf{R}'\mathbf{n}}(\mathbf{r})$ is similar to that of $F(\mathbf{r})$, which means that the operator $[\tilde{\varepsilon} - (H - \alpha P_v)I]^{-1}$ has very narrow spread in the real space.
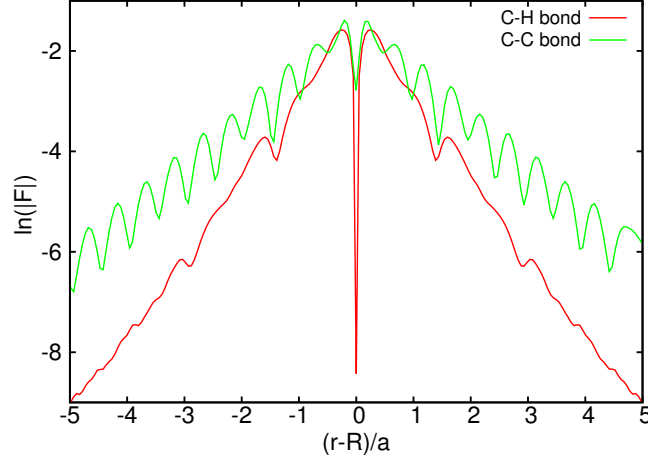

FIG. S3: The exponential decay of $F(\mathbf{r})$, which results from the locality of both Wannier functions and the density matrix.

On the other hand, the decay behavior of $||\Delta W_{\mathbf{R}n,\mathbf{R}'n'}||$ is dominated by the hopping term, $\tilde{\varepsilon}_{\mathbf{R}n,\mathbf{R}'n'}$. We show the exponential decay of $\tilde{\varepsilon}_{\mathbf{R}n,\mathbf{R}'n'}$ in Fig. S4a, and the strong correlation between $\tilde{\varepsilon}_{\mathbf{R}n,\mathbf{R}'n'}$ and $||\Delta W_{\mathbf{R}n,\mathbf{R}'n'}||$ in Fig. S4b.
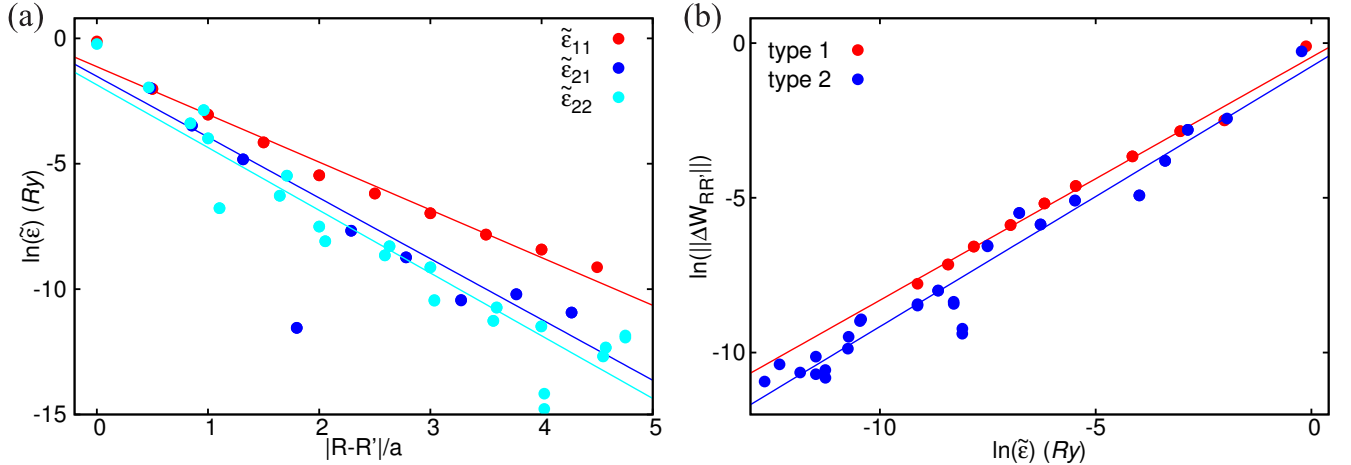

FIG. S4: (a) The exponential decay of the Hamiltonian matrix in the Wannier basis. (b) The strong correlation between the magnitude of the local response and the hopping terms suggests that the rapid decay of the charge-flow is due to the decay of hopping terms between different WFs.

SCALING ANALYSIS OF χ^0

In this section, we derive the numerical scaling to compute χ^0. We will only consider the static limit, as the computational cost to calculate χ^0 at an imaginary frequency follows the same scaling. Here we focus on the computationally challenging case of non-periodic extended systems. The computational model normally contains a large number of electrons, N, in a super cell. For this reason, we consider only the Γ-point in the Brillouin zone, and drop $\mathbf{k}$ and $\mathbf{q}$ in the notation. Under the plane-wave implementation, suppose such a system has N_v occupied states and N_c unoccupied states at a given kinetic energy cutoff. The number of occupied Wannier orbital, N_w, is the same as N_v. The size of the plane-wave grid is denoted by N_G. Here and in the following we use capital N for variables that scale with the system size, and use lower case n for variables independent of the system size.

The most straightforward way to compute χ^0 is to use the Adler-Wiser formula [4, 5]:

$$\chi^0_{\mathbf{G},\mathbf{G}'} = \frac{1}{\Omega} \sum_{ij} (f_i - f_j) \frac{\langle i|e^{-i\mathbf{G}\cdot\mathbf{r}}|j\rangle \langle j|e^{i\mathbf{G}'\cdot\mathbf{r}'}|i\rangle}{\varepsilon_i - \varepsilon_j + i\eta}. \tag{1}$$

For semiconductors and insulators, Eq. 1 requires $N_v \times N_c$ Fast Fourier Transforms to calculate all pairs of co-density $\psi_i^*(\mathbf{r})\psi_j(\mathbf{r})$ in the G space, whose cost is proportional to $N_v \times N_c \times N_G ln N_G$. Evaluating the full matrix of χ^0 requires four loops for $\mathbf{G}, \mathbf{G}', i$, and j, so the leading order of the scaling is $O(N^4)$. Besides, the direct approach needs to store N_G^2 elements. Both the computational and storage expenses become major bottlenecks for large systems.

Alternatively, as illustrated in the main text, we could represent χ^0 in a local basis set, $\{|\xi_i^n\rangle\}$, made of approximate eigenmodes of local response. $|\xi_i^n\rangle$ refers to the i-th approximate eigenvector of the local response of the n-th WF, χ^0_{nn}. If we need n_m eigenmodes for each WF, the cost of the storage is proportional to $n_m \times N_w \times N_G$. Since n_m is independent of the system size, the cost to store χ^0 grows as $O(N^2)$, but with a much smaller prefactor as compared to the direct evaluation of the Adler-Wiser formula.

Now we analyze the computational cost of the local basis set approach. In general $\{|\xi_i^n\rangle\}$ are obtained by iteratively solving the generalized Sterheimer equation and update ΔV_s for several times (typical in the order of ten), until the new ΔV_s is an eigenstate of χ^0. The matrix form of this equation reads:

$$\begin{pmatrix} \tilde{\varepsilon}_{0,0} - H & \cdots & \tilde{\varepsilon}_{0,N_w} \\ \vdots & \ddots & \vdots \\ \tilde{\varepsilon}_{N_w,0} & \cdots & \tilde{\varepsilon}_{N_w,N_w} - H \end{pmatrix} \begin{pmatrix} \Delta W_0 \\ \vdots \\ \Delta W_{n_w} \end{pmatrix} = \begin{pmatrix} P_c \Delta V_s W_0 \\ \vdots \\ P_c \Delta V_s W_{n_w} \end{pmatrix}. \tag{2}$$

We construct the local basis set by removing the off-diagonal elements of $\tilde{\epsilon}$, and solve the eigenvectors of

$$(\tilde{\varepsilon}_{i,i} - H)\Delta W_i = P_c \Delta V_s W_i. \tag{3}$$

To apply projector $P_c = I - \sum_i |W_i\rangle\langle W_i|$ in principle requires $N_v \times N_G$ operations, however, we can benefit from the exponential locality of W_i, and truncate the summation of the Wannier centers to n_n neighbors within a properly chosen cutoff distance of the local perturbation without losing accuracy. The computational cost to calculate the right hand side of Eq. 3 therefore scales as $n_n \times N_G$, and the iterative solution of ΔW_i scales as $N_G \ln N_G$. The cost to construct the full local basis set will acquire a prefactor of $n_m \times N_w$, which gives an overall $O(N^2)$ scaling.

To compute $X_{ij}^{nn'} = \langle \xi_i^n|\chi^0|\xi_j^{n'}\rangle$ used in the dielectric band structure interpolation, one has to solve N_w coupled equations in Eq. 2. Again, thanks to the exponential localization of χ^0, only n_n coupled equations needs to be solved for each $|\xi_j^{n'}\rangle$. Therefore the leading cost to construct X is n_n times of the cost of building the basis set, which again grows as $O(N^2)$. Compared to the $O(N^4)$ scaling of the standard Adler-Wiser formula, the local basis set approach has a tremendous saving in both computer time and memory.

---

[1] A. A. Mostofi *et al.*, Computer Physics Communications **178**, 685 (2008).
[2] P. Giannozzi *et al.*, J. Phys.: Condens. Matter **21**, 395502 (2009).
[3] J. P. Perdew and A. Zunger, Phys. Rev. B **23**, 5048 (1981).
[4] S. L. Adler, Phys. Rev. **126**, 413 (1962).
[5] N. Wiser, Phys. Rev. **129**, 62 (1963).